MODELING OF KINETICS OF MACROCHANNELING OF FAST ELECTRONS AND IONS IN PLANAR GAP COLLIMATORS

S.V. Dyuldya*, M.I. Bratchenko, M.A. Skorobogatov

National Science Center "Kharkov Institute of Physics and Technology", 61108, Kharkov, Ukraine

(Received May 23, 2006)

Using the novel method of macroscopic computer simulation of the reflection of charged particles from solid surfaces at grazing incidence the kinetics of planar macrochanneling, the directed transport of particles between surfaces separated by macroscopic distance, has been studied for swift electrons and ions. The dechanneling functions at macrochanneling have been calculated for the first time. The modeling of angular distributions of particles has confirmed the effect of beam angular splitting at the exit of macrochannel. The method of the taking into account of surface atomic discreteness at modeling of coherent effects of ion planar semichanneling has been developed. It has been shown that due to stochastic effects of particles reflection the macrochanneling of electrons in long channels is actually reduced to the effects of beam collimation while for ions the coherent effect allows to stabilize the macrochanneling and to achieve the beam transportation at long distances without considerable losses of intensity.

1. INTRODUCTION

Macrochanneling, the steered motion of charged particles between deflective solid surfaces separated by macroscopic distance, is the macroscopic analogue of the particles' channeling in single crystals. The effect had been discovered experimentally [1] in course of investigations of the penetration of MeV energies electron beams through targets with extended inhomogeneities.

Unlike for the bulk channeling in crystals that is controlled by continuum potentials of atomic planes and/or chains [2] the basic event forming the macrochanneled particles trajectories is the reflection from solid surface. It has large probability at grazing incidence and, depending on the sort of particle, the state of surface and the angle of beam incidence, can be originated either from multiple atomic collisions of a particle inside the near-surface region or from the scattering by surface atoms.

Due to the fact that between successive reflection events particles move in a free space without scattering the macrochanneling is supposed to provide the beam transport at large distances with small energy losses [3, 4]. Similarly, the transport through bent macrochannels or collimators of appropriate geometry can lead to the relativistic beams turning [3, 5], splitting or focusing.

These applications stimulate the interest to the effect both from the point of view of the development of the accelerator related beam shapers and irradiation devices as well as of the progress of experimental technique in high energy physics. The studies of macrochanneling can also clarify certain aspects of particle channeling in nanotubes [6] that in fact occupies an intermediate position on the scale of transversal dimensions of channels.

However no attempts can be found in the literature to build the quantitative kinetic theory of the effect. In the present paper the kinetics of macrochanneling of relativistic electrons and fast ions in planar gap collimators is studied using the "macroscopic" computer simulation of multiple reflections of particles from solid surfaces. The work is based on the novel simulation method developed in Ref. [7].

2. MODELING METHODS

For any definite geometry the modeling of macrochanneling *per se* comes to the following iterative procedure: the modeling of reflection event alternates to the 3D geometric calculation of the particle free motion between its collisions with surfaces. The latter can be easily carried out using the ray tracing algorithms while the main problem consists in the development of adequate and computationally effective methods of the simulation of the small-angle surface scattering.

Currently the charged particles' backscattering from solid surfaces is well studied both experimentally and theoretically either for ions [8, 9] or for swift electrons [10]. The reflection coefficient R (integral albedo) typically decreases with the increase of particle energy E but increases with the reduction of the angle ψ_{in} between the beam axis and the surface plane (see Fig. 1).

---

*Corresponding author. E-mail address: sdul@kipt.kharkov.ua

90

PROBLEMS OF ATOMIC SCIENCE AND TECHNOLOGY, 2007, N5.
Series: Nuclear Physics Investigations (48), p.90-97.

As ψ_{in} decreases the angular spectra of backscattered particles demonstrate the transformation from the cosine-shaped distributions for normal incidence toward the distributions concentrated near the direction of specular reflection. For heavy particles (ions) and for electrons at sufficiently high energies (that allow to neglect quantum diffraction effects) this behavior can be described within the scope of conventional mechanism of particle backscattering due to the sequence of uncorrelated (incoherent) atomic collisions. The target lattice structure is completely neglected in these models and the reflection mechanisms are only graded by the multiplicity of atomic scattering events that yield to the backscattering. For normal incidence major contribution is given by single strong Rutherford scattering while for grazing incidence ($\psi_{in} \ll 1$) substantial contribution is due to the multiple small-angle scattering that is described by boundary problems of kinetic equations of Fokker-Planck type [10].
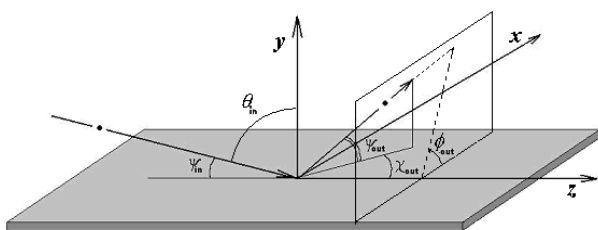

Fig.1. *The geometry of small-angle reflection of particles from the solid surface. Indicated are the incident ($\psi_{in} = 90° - \theta_{in}$) and emergency ($\psi_{out}, \chi_{out}, \phi_{out}$) angles that describe the backscattering event*

Qualitatively the mechanisms of small-angle backscattering at grazing incidence are described by the non-dimensional parameters σ^* and σ [10].

The scattering parameter:

$$\sigma^*(E) = \frac{R_0(E)}{l_{tr}(E)} \qquad (1)$$

is the ratio of particle range R_0 and the transport scattering length $l_{tr} = [n \cdot \sigma_{tr}(E)]^{-1}$ where n is the target atomic concentration, $\sigma_{tr} = 2\pi \int (1 - \cos\theta) d\sigma_{el}(\theta)$ is the transport cross-section, $d\sigma_{el}/d\theta$ is the differential cross-section of elastic scattering. The greater is σ^* the stronger is scattering as compared with stopping.

Integral albedo R, angular distributions and energy spectra of reflected particles are qualitatively determined by the non-dimensional reflection parameter σ:

$$\sigma(E, \psi_{in}) = \frac{\sigma^*(E)}{1 - \cos\psi_{in}} \approx \frac{R_0(E) \cdot \langle\theta_{MS}^2(E)\rangle}{\psi_{in}^2}, \quad (2)$$

where $\psi_{in} \ll 1$ and $\langle\theta_{MS}^2(E)\rangle$ is the mean squared angle of multiple scattering per unit of range. Large $\sigma \gg 1$ causes large $R \to 1$ and quasi-elastic reflection. The total albedo $R(E, \psi_{in})$ for arbitrary angle of incidence is represented by the weighted sum of small-angle ($R_1(E, \psi_{in})$) and diffuse ($R_2(E, \psi_{in})$) backscattering coefficients:

$$R \approx R_1 + (1 - R_1) \cdot R_2. \qquad (3)$$

In Ref. [10] explicit parametrizations of $R_{1,2}(E, \psi_{in})$ functions are given; one should note that the reflecting material's properties in these formulae are expressed only via the values of reduced parameters σ^* and σ.

The correlated energy-angular distribution of reflected particles is described by the expression [10]:

$$R_{\psi\chi\Delta}(\psi_r, \chi_r, \Delta) = \frac{2\sqrt{3} \cdot \psi_r}{(\pi\sigma\Delta)^{3/2}\Delta} \cdot \mathrm{erf}\left(2\sqrt{\frac{3\psi_r}{\sigma\Delta}}\right)$$
$$\times \exp\left[-\frac{4}{\sigma\Delta} \cdot \left(\psi_r^2 - \psi_r + 1 + \frac{\chi_r^2}{4}\right)\right], \quad (4)$$

where $\psi_r = \psi_{out}/\psi_{in}$, $\chi_r = \chi_{out}/\psi_{in}$, and $\Delta = (E - E_{out})/E$ is the normalized energy loss.

The equations (3–4) are universal in the meaning that they describe the incoherent reflection of either light or heavy particles of high energies provided the scattering parameter σ^* is calculated properly according to the definite laws of their stopping and scattering.

In Ref. [7] we have developed the Monte Carlo method of sampling of angular and energy variables from the distribution (4). Along with the sampling of reflection event with the probability (3) this method allows efficient modeling of multiple reflections of particles at macroscopic level (i.e. without the requirement to model microscopic atomic collisions). Below this method is applied to the Monte Carlo simulation of macrochanneling of electrons as well for that of ions at sufficiently large ψ_{in}. The method enhancements developed in order to describe coherent effects of surface semichanneling of ions at smaller ψ_{in} are introduced in Section 4.

We limited ourselves with the case of planar macrochannel (collimator) formed by parallel surfaces of Copper separated by the distance w_{ch}=3 mm that is much smaller then the lateral dimensions of the device. For simplicity the surface roughness was neglected and it was treated as a geometrical plane. In calculations the macroscopic length L of the collimator was varied in a broad range from 10 mm up to 2 m.

For each modeling case more then 10^6 histories of primary particles have been sampled. It allowed us to score both integral and differential characteristics of macrochanneling with acceptable statistical accuracy.

We considered expedient to describe the macrochanneling within the scope of the same kinetic concept that is accepted in the conventional theory of channeling in crystals. Hence we have introduced the dechanneling function $P_{ch}(z)$ that represents the probability to find moving particle at depth z of beam transport through the channel. Evidently $P_{ch}(0) = 1$ while $T = P_{ch}(L)$ is the macrochannel transmittance factor (the transparency).

Other quantities under investigation were the statistics of particle reflections from the walls of channel and angular distributions of particles passed through it. In toto this gives the complete description of the effect and allows us to make conclusions concerning its mechanisms and the peculiarities of its practical applications.

3. PLANAR MACROCHANNELING OF RELATIVISTIC ELECTRONS

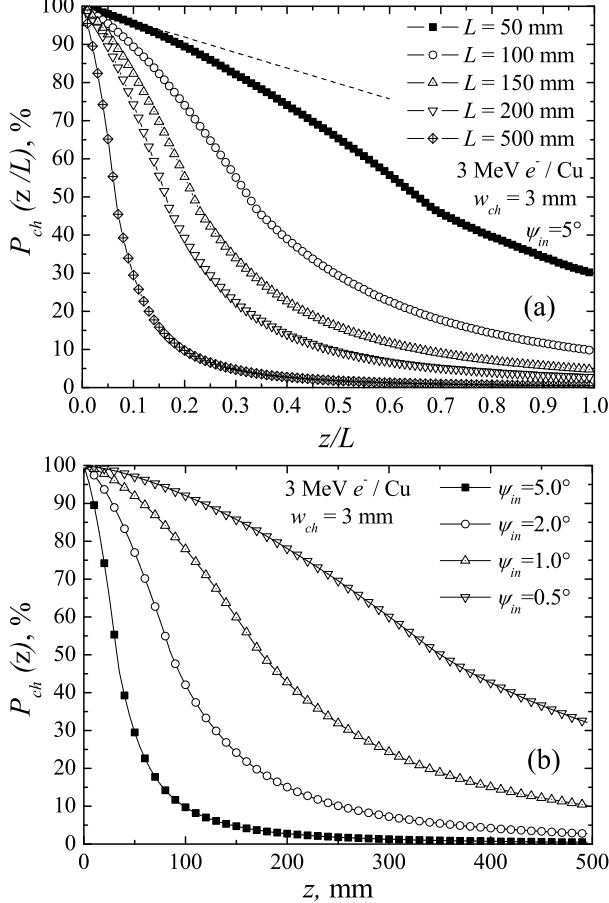In Fig.2 the obtained macro-dechanneling functions of 3 MeV monodirectional electron beam are shown.

Fig.2. *Dechanneling functions of relativistic electrons in planar macrochannels of different length L (a) and at different incident angles ψ_{in} at the entrance (b)*

According to Eqs. (1-2) for $E=3$ MeV the scattering parameter $\sigma^* = 2.55$ and for $|\psi_{in}| = 5°$ the reflection parameter $\sigma = 670 \gg 1$. Thus the reflection is close to elastic one but has comparatively broad angular distribution near the specular reflection angle $|\psi_{out}| = |\psi_{in}|$.

The characteristic length that describes the depth dependencies at macrochanneling is the distance z between successive collisions with surfaces:

$$\Delta z(\psi) = \frac{w_{ch}}{\tan\psi} \approx \frac{w_{ch}}{\psi}. \qquad (5)$$

At fixed ψ it estimates the half-wavelength of zigzag trajectory; note that in our case $\Delta z(5°) = 34.3\,mm$.

The curves of Fig.2,a are plotted at fixed ψ_{in} versus the reduced depth (z/L) and in fact demonstrate different stages of the same depth dependence. It is clear that the behavior of the dechanneling function considerably changes with the increase of the depth as compared with Δz. At small $z < \Delta z(\psi_{in})$ where the points of first collisions with surface are distributed the dechanneling function decreases rapidly due to the absorption of particles by the channel wall. In our case of the single surface collision albedo $R(5°) = 0.72$ the small-depth asymptotic form of $P_{ch}(z)$:

$$P_{ch}(z) \approx 1 - [1 - R(\psi_{in})] \cdot \frac{z}{\Delta z(\psi_{in})} \qquad (6)$$

demonstrates much slower decrease then the rate observed in modeling (see the dashed line in Fig.2,a). It means that even at $z < \Delta z(\psi_{in})$ multiple surface collisions of particles can take place due to the deviation of the reflection law from the specular one.

At $z \approx \Delta z(\psi_{in})$ the dechanneling function has the discontinuity of derivative and the rate of decrease of $P_{ch}(z)$ is considerably reduced. According to the intuitively obvious model of specular reflection with constant absorption probability $A(\psi_{in}) = 1 - R(\psi_{in})$ the dechanneling function becomes exponential at large z:

$$P_{ch}(z) = \exp\left(-\frac{z}{R_{ch}}\right); \ \ R_{ch} = \frac{w_{ch}}{\ln R^{-1} \cdot \tan\psi_{in}}. \qquad (7)$$

Here R_{ch} has the meaning of dechanneling length.

However the calculation of $R_{ch}(z) = -z/\ln P_{ch}(z)$ according to the modeled $P_{ch}(z)$ data has shown that at large z the dechanneling length increases with depth; therefore the dechanneling function decreases slower then the exponent. This fact is also due to the non-specular mode of backscattering: certain part of electrons reflects at angles $|\psi_{out}| < |\psi_{in}|$ and their length of free motion between successive reflections increases as compared with $\Delta z(\psi_{in})$. Just these particles form the long-range non-exponential tail of dechanneling function.

The directional dependence of the dechanneling function shown in Fig.2,b for the macrochannel of fixed length $L = 500$ mm indicates that at smaller incident grazing angles ψ_{in} electrons are transported in the macrochannel more effectively. Mainly it is due to the increase of free path length between the walls (that is proportional to ψ^{-1}) and to the corresponding decrease of the number of collisions with surfaces.

The distributions of the number N_{refl} of reflection events shown in Fig.3 indicate that at large L it becomes substantially smaller then the asymptotic estimation $N_{refl} \approx (L \cdot \tan\psi_{in})/w_{ch}$ that follows from the simple specular reflection model (in this model at $\psi_{in} = 5°$, $N_{refl} \sim 3$ for $L=100$ mm and approaches to 14 for $L=500$ mm).

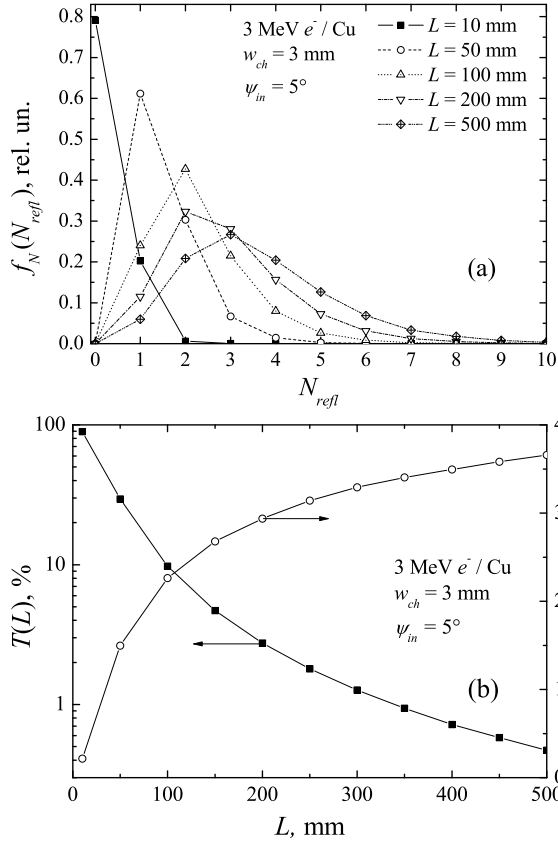**Fig.3.** *The distributions of electrons over the number N_{refl} of reflection events (a) and the dependencies of the transmittance factor T and the mean number of reflections $\langle N_{refl} \rangle$ (b) in collimators of various lengths*

The rate of increase of the mean number $\langle N_{refl} \rangle$ substantially reduces with the increase of L and $\langle N_{refl} \rangle$ practically saturates to the value of 4 at large L (in the specular reflection model the value $N_{refl} \approx 4$ corresponds to $L \approx 140\,mm$). Accordingly, the transmittance factor T becomes marginal at large $L \gg \Delta z(\psi_{in})$.

Therefore one can conclude that for relativistic electrons the deviation of reflection probability R from unity and the non-specular mode of backscattering substantially restrict the range of depths where the particles dynamics looks like the quasi-periodic motion between the walls (that is peculiar to the planar channeling in crystals). At large L macrochannels operate as conventional collimators where the transmittance factor is determined only by the geometric ratio of width and length.

This conclusion agrees with the results of the modeling of fine structure of angular distributions of electrons at the exit of macrochannels of various lengths. These results are illustrated by Figs. 4 and 5.

At sufficiently small L the maps of angular distributions of Fig.4,a-c are essentially asymmetric in the vertical direction that corresponds to the emergency angle ψ_{out} with respect to the channel wall.

At $L=10$ mm that is less then $\Delta z(\psi_{in})$ about 80% of electrons pass the channel without collisions with surfaces (their contribution shrinks to the point at the vertical axis of lower half plane of Fig.4,a).

The residuary 20% of electrons form a typical angular distribution of single backscattering at grazing incidence [10, 7].
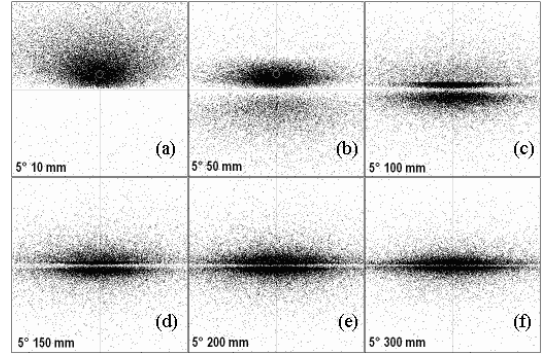

Fig.4. *The maps (projected onto the transversal plane of planar macrochannel) of angular distributions of 3 MeV electrons passed through the macrochannels of various length L at the angle of incidence $\psi_{in} = 5°$. The center of gray circle with angular aperture 20 mrad (1.15°) indicates the direction of specular reflection of particles from the lower wall of macrochannel*
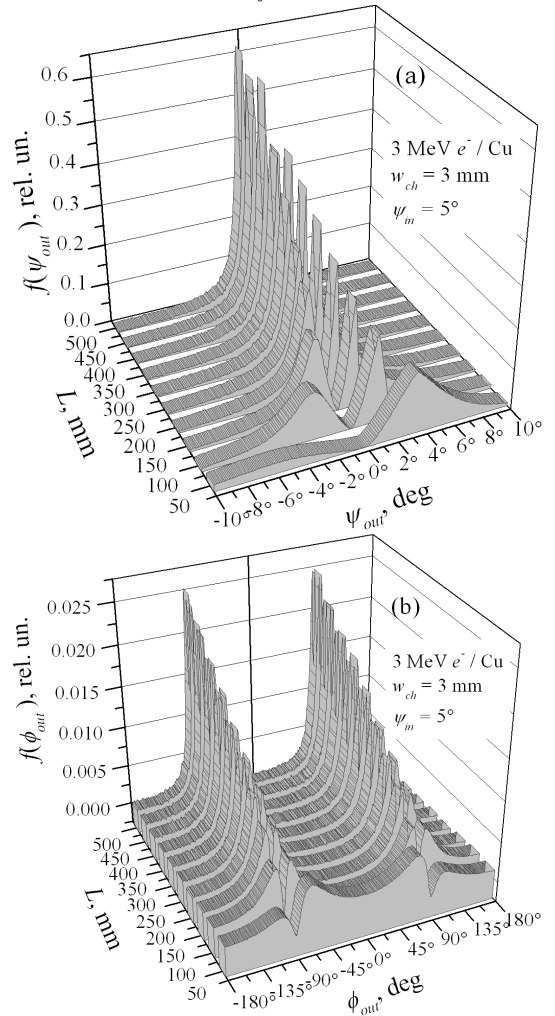

Fig.5. *The angular distributions of 3 MeV electrons passed through the macrochannels of different length L over the grazing emergency angle ψ_{out} to the channel wall (a) and the azimuthal angle ϕ_{out} in the transversal plane (b, $\phi_{out} = 0°$ corresponds to the beam incidence plane)*

As L increases the contribution of electrons that have experienced even numbers of reflection events arises; they form the distribution in the lower half plane of angular maps. At the same time the flux of electrons having odd numbers of reflections and emerging in the upper half plane is hardly collimated.

At large L the angular distributions tend to become vertically symmetrical (see Fig.4,d-f).

The results of statistical analysis of obtained angular maps are shown in Fig.5. The data depicted in Fig.5,a demonstrate the effect of beam angular splitting first observed experimentally in Ref. [1].

The effect consists in the reduction of the transmittance of a planar macrochannel in directions parallel to its walls. On the angular maps of Fig.4,c-f the splitting manifests itself as a clear band close to the horizontal axis $\psi_{out} = 0$ and is tracked up to large lengths of macrochannels.

The separated peaks in angular distributions over the grazing angle ψ_{out} are formed by electrons experienced even and odd numbers of surface collisions.

The positions of angular peaks are rather close to the collimation angle $\psi_{col} = w_{ch}/L$ of the macrochannel.

Azimuthal distributions of electrons depicted in Fig.5,b describe the gradual unfolding of a beam in the lateral plane of the macrochannel and its localization nearby the directions $\phi_{out} \to \pm 90°$ parallel to the channel walls (however the directions $\phi_{out} = \pm 90°$ themselves remain blocked due to the same splitting effect).

Hence in long planar gaps the monodirectional beam transforms into the ribbon-type one rotated azimuthally by 90°. This effect is peculiar to planar geometry only; in macrochannels of other shapes (e.g. square or cylindrical) azimuthal distributions are more axially symmetric.

4. COHERENT EFFECTS IN PLANAR MACROCHANNELING OF IONS

Macrochanneling of positively charged particles (protons, heavy ions or positrons) differs qualitatively from the marcochanneling of electrons due to the fact that it can be affected by coherent effects of correlated interaction of particles with surface plane [4, 5]. Similarly to the description of planar channeling in crystals this interaction can be described with the repulsive continuum surface potential $U(y)$ that depends only on the distance y to the surface. The continuum potential can be introduced not only for crystalline surface but also for planar surface of amorphous medium [11].

If the grazing angle ψ_{in} of a positively charged particle does not exceed the critical angle $\psi_p = \sqrt{U_p/E}$ of planar channeling [2] (here $U_p = 2\pi Z_1 Z_2 e^2 a_{TF}/a^2$ is the surface potential barrier, $Z_{1,2}$ are the atomic number of incident particle and target medium with the mean interatomic distance a, a_{TF} is the Thomas-Fermi screening length) then due to the

homogeneity of $U(y)$ along the surface the transversal energy of reflected particle is conserved. Thus the specular reflection occurs that is due to coherent interaction of a particle with surface atoms with strong correlation of impact parameters. This mode of backscattering, the planar surface semichanneling, has dynamical (but not kinetic) nature and can facilitate the beam transportation in long macrochannels. Obviously for $\psi_{in} \geq \psi_p$ surface semichanneling becomes impossible and the reflection mode returns to the incoherent one that is described by the distribution (4).

However it must be taken into account that even for $\psi_{in} < \psi_p$ stochastic deviations of surface potential from the averaged $U(y)$ lead to incoherent multiple scattering that results in the non-conservation of transversal energy. In the bulk of crystals this factor causes the dechanneling; for surface scattering it results in non-specular reflection and has to be introduced into models designed to describe the ion macrochanneling quantitatively.

The dominating dechanneling factor at planar channeling of ions is the discreteness of atomic plane [2]. The mean-squared angles of incoherent multiple scattering per unit of range z of a particle that moves at distance y from the discrete atomic plane with randomly distributed atoms were estimated in Ref. [12].

For the standard Lindhard potential of particle-atom interaction [2] the orthogonal (y-) and lateral (x-) components of this quantity can be written as follows:

$$\left\langle \frac{\Delta\theta_y^2}{\Delta z} \right\rangle = \frac{45\psi_p^4}{64\pi} \frac{a^2 a_{TF}^2}{y^5}; \quad \left\langle \frac{\Delta\theta_x^2}{\Delta z} \right\rangle = \frac{1}{5} \left\langle \frac{\Delta\theta_y^2}{\Delta z} \right\rangle.$$
(8)

To estimate the mean-squared angle $\left\langle \Delta\theta^2 \right\rangle$ of incoherent scattering per single reflection event one has to integrate the expressions (8) upon the trajectory $y(z)$ of unperturbed motion governed by the continuum surface potential. The simplest analytical estimation follows from the "corner-type" trajectory representation:

$$y(z) = y_{min}(\psi) + |z| \cdot \psi,$$
(9)

where y_{min} is the distance of the closest approach of the particle to the surface. For the Lindhard continuum potential $y_{min}(\psi) \approx 1.5 \cdot a_{TF} \cdot (\psi/\psi_p)$. Then the y-component of variance is expressed by the formula:

$$\sigma_y^2 = \left\langle \Delta\theta_y^2 \right\rangle = \frac{45\psi_p^4}{128\pi} \frac{a^2 a_{TF}^2}{y_{min}^4(\psi) \cdot \psi} = \frac{5}{72\pi} \frac{a^2}{a_{TF}^2} \psi^3$$
(10)

and, again, the x-component is 5 times smaller. Within this model $\sigma_{x,y}$ only depend on the sorts of particle and target material and on the angle of incidence while do not depend on particle energy. One should note that the ratio $(\sigma_y/\psi_p)^2 \propto \psi^3$. Hence

the conditions of coherent specular reflection at planar semichanneling are improved as the grazing angle of incidence decreases. At critical value $\psi = \psi_p$ they are also improved with the increase of particle energy (because $\psi_p \propto E^{-1/2}$).

At our Monte Carlo modeling of ion macrochanneling for $\psi < \psi_p$ the emergency angles of backscattering around the direction of specular reflection were sampled from the normal distribution with zero mean value and variances $\sigma_{x,y}$ obtained above; we also accepted that $R(\psi < \psi_p) = 1$ and neglected the particle energy losses. At $\psi > \psi_p$ the same algorithm of incoherent reflection was applied that has been used for electrons.

To clarify the role of coherent effects we also considered the case of pure incoherent reflection of ions; for such a purpose we formally set $\psi_p = 0$.

The case of macrochanneling of 1 MeV protons in the same Copper collimator geometry described in Section 3 was considered. For this case the critical angle ψ_p of planar surface semichanneleng equals to $0.5°$.

For the evaluation of reduced parameters σ^* and σ according to Eqs. (1)-(2) the proton range $R_p = 6.8$ μm had been obtained using the *SRIM* code. Combining this value with the value of the transport cross-section σ_{tr} calculated within the Firsov model [10] we have calculated the scattering parameter $\sigma^* = 0.017 \ll 1$. It means that these protons effectively reflect from the surface only at grazing incidence. However at $\psi_{in} = 0.4°$ the incoherent reflection parameter (2) for 1 MeV protons $\sigma \approx 700 \gg 1$ is close to the value $\sigma \approx 670$ for 3 MeV electrons at $\psi_{in} = 5°$, the case discussed in Sec.3.

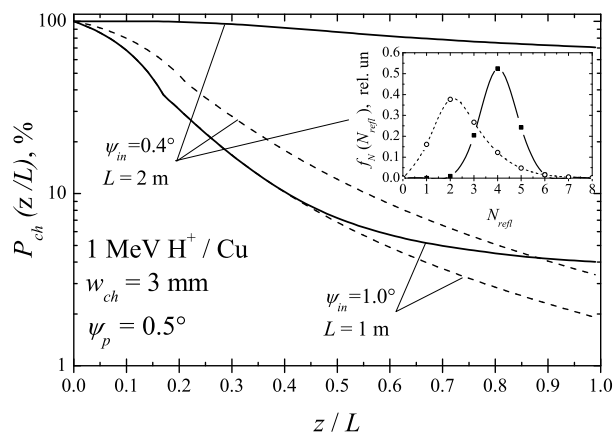The effect of the coherent reflection mode on the dechanneling functions is illustrated by Fig.6.

Fig.6. Dechanneling functions of 1 MeV protons in Copper macrochannels of different lengths with (solid curves) and without (dashed curves) the account of coherent reflection (planar surface semichanneling) mechanism. The inset plot represents the particle distributions over the number N_{refl} of reflection events

At conditions of a sub-barrier incidence of protons ($\psi_{in} = 0.4° = 0.8 \cdot \psi_p$) the effect of coherent reflection

at planar surface semichanneling is very strong: the 2 m long macrochannel transmits about 70% particles while for pure incoherent reflection mode the transmittance factor is less then 4%. The most probable number of reflection events in the case of semichanneling shifts toward the theoretical estimation of specular reflection model: $N_{refl} \sim L \cdot \psi_{in}/w_{ch} \approx 4.65$.

In the case of above-barrier incidence of particles ($\psi_{in} = 1° = 2 \cdot \psi_p$) the effect of volume capture of protons into the mode of surface semichanneling is observed. This effect results in sharp deceleration of the $P_{ch}(z)$ dependency starting from the depth $z \approx 60$ cm.

Angular distributions of ions (see Fig.7 and 8) also demonstrate strong qualitative effects of coherent reflection. At sub-barrier incidence (see Fig.7,a,d) the introduction of surface semichanneling leads to drastic changes of the distribution: the symmetrical gauss-shaped spots appear. As it is clear from Fig.8,a they are close to the specular reflection directions $|\psi_{out}| \approx 0.4°$ and are formed by well-channeled protons. Azimuthal distribution over ϕ_{out} depicted in Fig.8,b also indicates the concentration of coherently transported protons nearby the incidence plane ($\phi_{out} = 0°$ and $\pm 180°$). Horizontal bands in Fig.7,d are formed by dechanneled particles that have experienced the incoherent reflection.

If coherent effects are completely ignored the distribution in this case is qualitatively similar to the angular distribution of electrons at large L (see Fig.4).

At conditions of above-barrier proton incidence (see Fig.7,b,e) the characteristic effect of surface semichanneling consists in the splitting of angular distribution in the upper half plane of transversal angular map. It indicates the separated contributions of proton flux fractions that are either incoherently backscattered or captured into the coherent reflection mode.

The formation of gauss-shaped spots is suppressed in this case because particles have time to experience substantial lateral scattering before the volume capture event occurs.
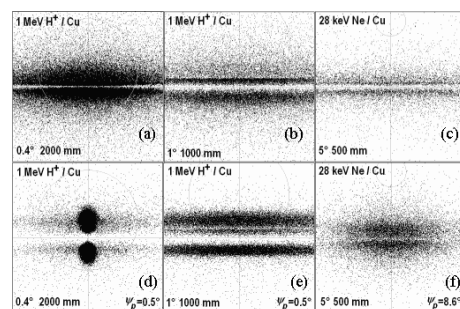

Fig.7. The maps of angular distributions of 1 MeV protons (a,b,d,e) and 28 keV Ne ions (c,f) passed through the 3 mm wide Copper macrochannels of different lengths at different angles of incidence. Upper maps describe the pure incoherent mode of reflection while the lower row of maps corresponds to the incorporation of the coherent surface semichanneling mode
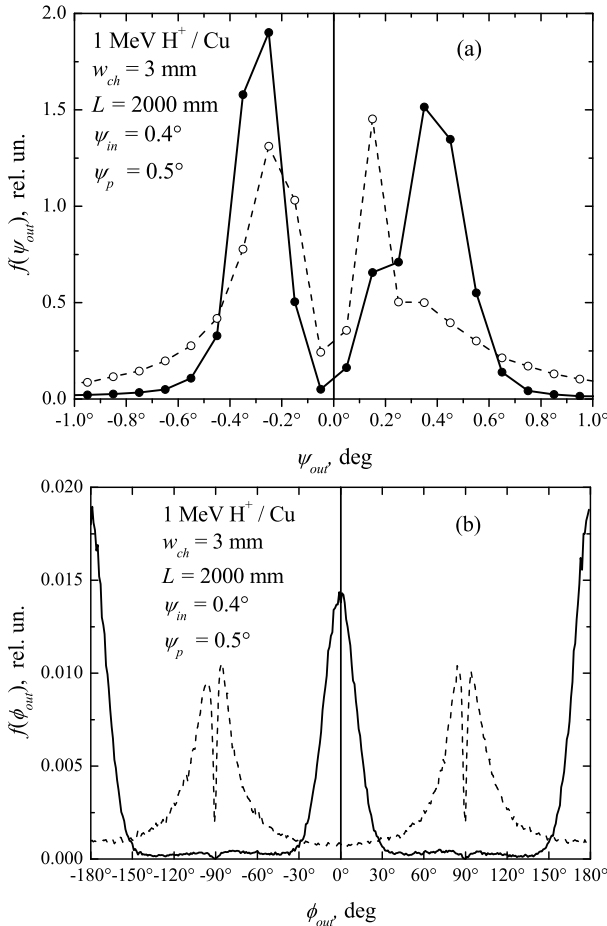
Fig.8. *Angular distributions over the grazing emergency angle ψ_{out} (a) and the azimuthal angle ϕ_{out} in the transversal plane (b) for protons passed through the 2 m long planar macrochannel. Dashed curves — incoherent reflection mode (see Fig.7a), solid curves — coherent surface semichanneling mode (see Fig.7,d)*

The data of Fig.7,c,f correspond to the case of macrochanneling of heavier ions (28 keV Ne) at sub-barrier incidence ($\psi_{in} = 5°$). In this case $\psi_p = 8.9°$, $\sigma^* = 1.2$, $\sigma \approx 315$. One can see that for heavy ions the effect of surface semichanneling is also remarkable. However due to large value of the incident angle ψ_{in} the destructive effect of surface atomic discreteness becomes very pronounced (this fact directly follows from Eq.(10)). Thus the incoherent multiple scattering results in the smearing of the spots of coherent reflection and in the relative increase of contributions of effects of geometrical collimation of ion beam.

5. CONCLUSIONS

The computer simulation has shown that the macrochanneling of relativistic negatively charged particles between the planar solid surfaces differs considerably from the regular oscillatory motion due to substantially stochastic nature of small-angle reflection of electrons at glancing incidence. In long channels it practically comes to the beam collimation within the angular range determined by the

channel geometry and makes questionable the long-range transportation of electron beams without significant losses of intensity. From the other hand the macrochannels of certain optimal length can be applied for electron beam angular splitting and for the enhancement of yields of secondary processes of particle-surface interactions.

It has been shown that for positively charged particles (ions or positrons) the coherent effect of surface semichanneling allows to stabilize the macrochanneling trajectories, to reduce the particle losses and to achieve the transport and splitting of high energy beams.

The methods of macroscopic mathematical modeling of the macrochanneling are supposed to be effectively applied for calculations of ion-optical systems that use the particles interaction with solid surfaces for beam control and shaping. For example one of the prospective areas of the macrochanneling applications is the preparation of small-diameter focused ion beams for the solid surface microanalysis.

REFERENCES

1. V.I. Bojko, V.V. Yevstigneyev, B.A. Kononov et al. Anisotropy of electron fluxes behind the extended inhomogeneities in medium // *Atomnaya energiya.* 1976, v.41, N5, p.363-365 (in Russian).

2. J. Lindhard. Influence of crystal lattice on motion of energetic charged particles // *Kgl. Dan. Viden. Selsk. Mat.-Fys. Medd.* 1965, v.34, N14.

3. V.I. Bojko, Ye.A. Gorbachov, V.V. Yevstigneyev et al. Turn and transportation of a beam of swift electrons based on macrochanneling effect // *JTP.* 1981, v. 51, N5, p.1042-1044 (in Russian).

4. M.A. Kumakhov. *Radiation of charged particles in crystals,* Moscow: "Energoatomizdat", 1986, 160p. (in Russian).

5. M.A. Kumakhov, F.F. Komarov. Reflection of particles and quanta from solid surfaces and regulation of their trajectories // *Radiation Effects.* 1985, v.90, N3-4, p.269-281.

6. N.K. Zhevhago, V.I. Glebov. Diffraction and channeling in nanotubes // *JETP.* 2000, v.118, N3, p.579-591 (in Russian).

7. S.V. Dyuldya, M.I. Bratchenko. Monte Carlo method of macroscopic modeling of small-angle reflection of fast changed particles from solid surface // *Problems of Atomic Science and Technology. Series: Radiation Damage Physics and Radiation Material Science.* 2001, N4(80), p.53-56 (in Russian).

8. V.A. Kurnayev, Ye.S. Mashkova, V.A. Molchanov. *Reflection of light ions from solid surface.* Moscow: "Energoatomizdat", 1985, 192p. (in Russian).

9. E.S. Parilis, N.Yu. Turayev, F.F. Umarov et al. *Theory of scattering of medium energies atoms by solid surface.* Tashkent: "Fan", 1987, 212p. (in Russian).

10. M.I. Ryazanov, I.S. Tilinin. *Surface studies by particle backscattering.* Moscow: "Energoatomizdat", 1985, 152p. (in Russian).

11. M.A. Kumakhov. The phenomenon of specular reflection of charged particles from amorphous and polycrystalline surfaces // *DAN USSR.* 1984, v.279, N4, p.862-863 (in Russian).

12. M.A. Kumakhov, H. Shirmer. *Atomic collisions in crystals.* Moscow: "Atomizdat", 1980, 192p. (in Russian).

МОДЕЛИРОВАНИЕ КИНЕТИКИ МАКРОКАНАЛИРОВАНИЯ БЫСТРЫХ ЭЛЕКТРОНОВ И ИОНОВ В ЩЕЛЕВЫХ КОЛЛИМАТОРАХ

С.В. Дюльдя, М.И. Братченко, М.А. Скоробогатов

Оригинальным методом макроскопического математического моделирования отражения заряженных частиц от поверхности твердого тела исследована кинетика плоскостного макроканалирования быстрых электронов и ионов — ориентированного транспорта частиц между поверхностями, разделенными макроскопическим расстоянием. Впервые рассчитаны функции деканалирования частиц при макроканалировании. Моделирование угловых распределений подтвердило существование эффекта разделения потоков частиц. Разработан метод учета атомной дискретности поверхности при моделировании когерентных эффектов плоскостного полуканалирования ионов. Показано, что ввиду стохастичности процесса отражения макроканалирование электронов в каналах большой длины эффективно определяется механизмами коллимации пучка, тогда как для ионов когерентный эффект позволяет стабилизировать макроканалирование и достичь транспортировки и разделения пучка на больших расстояниях без существенных потерь интенсивности.

МОДЕЛЮВАННЯ КІНЕТИКИ МАКРОКАНАЛЮВАННЯ ШВИДКИХ ЕЛЕКТРОНІВ ТА ІОНІВ У ЩІЛИННИХ КОЛІМАТОРАХ

С.В. Дюльдя, М.І. Братченко, М.О. Скоробогатов

Оригінальним методом макроскопічного математичного моделювання відбиття заряджених частинок від поверхні твердого тіла досліджена кінетика площинного макроканалювання швидких електронів та іонів — орієнтованого транспорту частинок між поверхнями, розділеними макроскопічною відстанню. Вперше розраховані функції деканалювання частинок при макроканалюванні. Моделювання кутових розподілів підтвердило існування ефекту розділення потоків частинок. Розроблено метод урахування атомної дискретності поверхні в моделюванні когерентних ефектів площинного напівканалювання іонів. Показано, що з-за стохастичності процесу відбиття макроканалювання електронів в каналах великої довжини ефективно визначається механізмами колімації пучка, тоді як для іонів когерентний ефект дозволяє стабілізувати макроканалювання та досягти транспортування та розділення пучка на великих відстанях без значних втрат інтенсивності.